Volatile anesthetic modulation of oligomerization equilibria in a hexameric model peptide

Giovanna Ghirlanda[a,b], Simon A. Hilcove[a,b], Ravindernath Pidikiti[c], Jonas S. Johansson[c,d], James D. Lear[d], William F. DeGrado[d], Roderic G. Eckenhoff[c,*]

[a] Departments of Biophysics and Biochemistry, University of Pennsylvania School of Medicine, Philadelphia, PA 19104, USA
[b] Department of Chemistry and Biochemistry, Arizona State University, Tempe, AZ 85287, USA
[c] Department of Anesthesia, University of Pennsylvania School of Medicine, 3620 Hamilton Walk, Philadelphia, PA 19104-6112, USA
[d] Departments of Biophysics, Biochemistry, and the Johnson Research Foundation, University of Pennsylvania School of Medicine, Philadelphia, PA 19104, USA

Received 4 October 2004; revised 29 October 2004; accepted 31 October 2004

Available online 16 November 2004

Edited by Takashi Gojobori

Abstract To determine if occupancy of interfacial pockets in oligomeric proteins by volatile anesthetic molecules can allosterically regulate oligomerization equilibria, variants of a three-helix bundle peptide able to form higher oligomers were studied with analytical ultracentrifugation, hydrogen exchange and modeling. Halothane shifted the oligomerization equilibria towards the oligomer only in a mutation predicted to create sufficient volume in the hexameric pocket. Other mutations at this residue, predicted to create a too small or too polar pocket, were unaffected by halothane. Inhaled anesthetic modulation of oligomerization interactions is a novel and potentially generalizable biophysical basis for some anesthetic actions.

Keywords: Halothane; Protein cavities; Anesthesia; Hydrogen exchange; Analytical ultracentrifugation

1. Introduction

Volatile anesthetics alter the activity of many biological targets through as yet poorly defined molecular mechanisms [1,2]. The lack of structural information, and the experimental difficulties in handling both the membrane proteins and the volatile anesthetics have thus far prevented the identification of anesthetic binding sites in all but a few such targets [3,4]. Water soluble proteins have therefore been popular model systems for studying anesthetic binding using X-ray crystallography [5,6], photoaffinity labeling [7] and fluorescence spectroscopy [8]. In general, volatile anesthetics bind to preorganized internal cavities with weak amphiphilic character, consistent with the strong correlation of anesthetic potency and hydrophobicity (Overton/Meyer) [2].

A haloalkane binding site was found at the interface between human serum albumin domains IIA and IIB [5], and at a domain interface in firefly luciferase [6]; in both cases, the native state of the protein is stabilized against unfolding by the haloalkane [9,10]. Thus, occupancy of interfacial sites could regulate protein activity allosterically through stabilization of domain/domain interactions. Extending these interdomain interactions to those of protein complexes, halothane promotes the oligomerization of SERCA1, the probable basis for the observed inhibitory activity of the Ca^{2+} pump [11,12], and induces co-localization on the membrane of the major histocompatibility complex proteins HLA I and II [13]. These observations could underscore a general mechanism of volatile anesthetics: modulation of oligomerization equilibria through occupancy of interfacial cavities.

We tested this general mechanism in a simple model system. A series of model proteins were previously designed to form hexameric complexes in solution [14]. These complexes are formed as three dimeric three-helix bundles, each with a leucine-rich hydrophobic core, and then further associate through an exposed aromatic patch on the surface to form the hexamer with an aromatic "supercore". The polarity and steric bulk of one of the aromatic residues in the supercore was mutated systematically to predictably modulate the stability of the hexamer. These mutations (from phenylalanine (Phe) to isoleucine (Ile), lysine (Lys) and alanine (Ala), respectively) also predict the formation of a cavity at the two extremities of the hexameric assembly that might accommodate a ligand. Molecular modeling suggests that the Ala mutant forms a hydrophobic cavity that can accommodate halothane (~120 Å^3), but in the Ile mutant, the cavity is too small, and in the Lys mutant, it is too polar and perhaps too small. Moreover, we hypothesized that anesthetic occupancy of the Ala mutant cavity would restore van der Waals contacts in the hydrophobic "supercore" of the assembly, and thus stabilize the hexameric form of the protein.

2. Methods

2.1. Molecular modeling

Computer models of the hexamers were generated from the crystal structure of the three-helix bundle, DSD (PDB entry 1G6U), using Insight II (Accelrys, Inc. San Diego, CA; www.accelrys.com) as described before [14]. Each three-helix bundle is formed by two chains of amino acids, numbered from 1 to 48 and from 1′ to 48′, respectively; the two other three-helix bundles in each hexameric assembly are referred to as B (B1–B48 and B1′–B48′) and C (C1–C48 and C1′–

*Corresponding author. Fax: +1 215 349 5078.
E-mail address: roderic.eckenhoff@uphs.upenn.edu (R.G. Eckenhoff).

0014-5793/$22.00
doi:10.1016/j.febslet.2004.10.087

C48′). Each mutant was energy-minimized using the Discover module within Insight II (cvff forcefield); for Hex-Lys, we built two different models in which different rotamer conformations were adopted for Lys 42 on each of the six chains. Because of the twofold symmetry in each dimer, identical putative ligand sites are located both at the top and bottom of the assembly; only one was evaluated by modeling. Each of the five models was screened for binding pockets using CASTp (http://cast.engr.uic.edu/cast/ [15]). This algorithm reports both the solvent (radius = 1.4 Å) accessible volume (SAV) [16] and molecular surface [17] volumes (MSV). We repeated the calculations with a probe radius close to the largest dimension of halothane (3.5 Å). Thus, any revealed pockets or cavities with non-zero SAV will accommodate halothane in any orientation. Further evaluation of halothane's occupancy employed the Docking module of Insight II. Briefly, a minimized model of halothane was manually placed in the cavity, and the fixed Docking program launched to search for optimal placement. For Hex-Ala the binding site comprised residues F28, A42′, L25, and E21 for each three-helix bundle (42′ is the mutated residue across the series). A multiple start was implemented so that bias from starting positions would be minimized. Of the four proteins, only Hex-Ala docked the halothane in an energetically favorable manner. Repeated simulations resulted in convergence of resultant structures towards an ensemble of halothane orientations within the cavity; in the conformation chosen, the interaction energy between the binding region and halothane was −5.3 kcal/mol.

2.2. Hydrogen–tritium exchange

Amide hydrogen exchange protection factors for "core" residues should be increased in the hexamer as compared to the dimer, so hydrogen–tritium exchange was used to monitor oligomerization. Peptide solutions (~5 mg/ml) were incubated with ~5 mCi ^{3}HOH in 1 M GdnCl, 0.1 M NaH_2PO_4, pH 8.5, buffer for 18 h at 23 °C; conditions intended to assure equilibration of all exchangeable hydrogens prior to initiation of exchange-out. Free ^{3}HOH was removed, buffer exchanged, and exchange-out initiated with a PD-10 gel filtration column (Sigma–Aldrich, St. Louis, MO). After recovery, the protein solution was transferred to pre-filled Hamilton (Reno, NV) gas-tight syringes containing halothane and equipped with repeaters. Aliquots were precipitated with 2 ml of ice-cold 10% trichloroacetic acid at timed intervals over at least 6 h. The precipitant was vacuum-filtered through Whatman GF/B filters (Clifton, NJ) and washed with 8 ml of ice-cold 2% TCA. Tritium retained by the protein was determined by liquid scintillation. Protection factor ratios (PFRs) were determined for the last 3–5 hydrogens in common for the two conditions (see figure legends), and $\Delta\Delta G$ was determined using $\Delta\Delta G = RT \ln(\mathrm{PFR})$.

2.3. Analytical ultracentrifugation

Hex-Ala and Hex-Lys samples ~75 μM protein in 100 mM Na Phosphate buffer at pH 7.0 containing either 0 or ~10 mM halothane were centrifuged to equilibrium at 35 (Hex-Ala) or 40 (Hex-Lys) KRPM in a Beckman XLI instrument using Yphantis-type carbon-epoxy cells. Radial concentration profiles were measured using interference optics with an effective extinction coefficient of 2.73 fringe-cm^3/mg. Data for the halothane-free Hex-Ala sample and for both Hex-Lys samples were fit to a monomer–trimer equilibrium considering the dimer to be the monomeric unit. Data obtained for the Hex-Ala sample in halothane-saturated buffer showed essentially complete trimerization of the dimer, precluding a measurement of the dissociation constant.

3. Results

3.1. Molecular modeling

In each of the three bundles, the residues identified as part of the cavity using the 1.4 Å probe were F28, A42′, L25, and E21 (highlighted in Fig. 1a (Hex-Ala) and 1b (Hex-Phe)) (Table 1). Only Hex-Ala displays a pocket large enough to accommodate halothane by both SAV and MSV methods; using the 3.5 Å probe, only the pockets in Hex-Ala had a non-zero SAV.

All the residues lining the cavity were included in the simulated docking calculations. Of the five models examined, only Hex-Ala showed a plausible result for the docking experiment: several simulations resulted in a convergent low-energy binding model (Fig. 2). The Hex-Ala/halothane complex was examined using the CASTp server in order to verify that the external ligand had efficiently filled the cavity; SAV of 80 Å^3 and MSV of 523 Å^3 were obtained. These values are comparable with those of the unliganded Hex-Phe and Hex-Ile mutants. The Hex-Ala mutant was therefore used to explore the effect of halothane binding on hexamer stabilization.

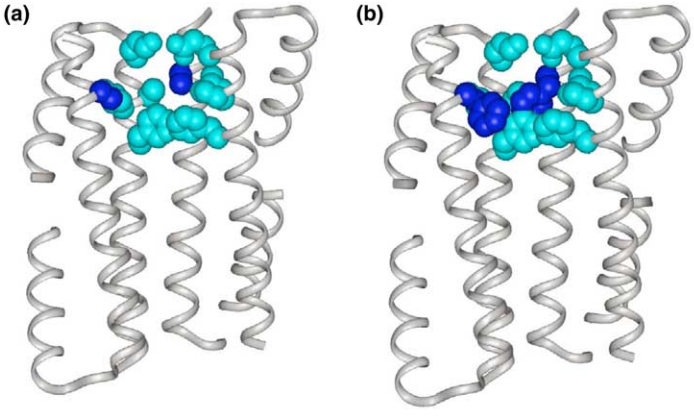

(c)

DSD	S	LAALKSE	LQALKKE	GFSPEE	LAALES**E**	LQALEK**K**	LAALKS**K** LQALKG
Hex-Phe	S	LAALKSE	LQALKKE	GFSPEE	LAALES**F**	LQALEK**W**	LAALKS**F** LQALKG
Hex-Ile	S	LAALKSE	LQALKKE	GFSPEE	LAALES**F**	LQALEK**W**	LAALKS**I** LQALKG
Hex-Ala	S	LAALKSE	LQALKKE	GFSPEE	LAALES**F**	LQALEK**W**	LAALKS**A** LQALKG
Hex-Lys	S	LAALKSE	LQALKKE	GFSPEE	LAALES**F**	LQALEK**W**	LAALKS**K** LQALKG

Fig. 1. Molecular models of two mutants, Hex-Ala (a) and Hex-Phe (b). For clarity, one of the three-helix bundles is omitted. Panel (c) shows the sequences of the four mutants investigated and of the starting dimeric three-helix bundle, DSD.

Table 1
CASTp results for each model in Å^2 (area) and Å^3 (volume) (shown are values for 1.4/3.5 Å probe radii)

Model	Surface area [16]	Surface area [17]	SAV [16]	MSV [17]
Hex-Phe	126/0	312/0	59/0	350/0
Hex-Ile	199/0	547/0	92/0	569/0
Hex-Ala	306/6	575/238	232/1	809/331
Hex-Lys	100/0	289/0	37/0	279/0
Hex-Lys 2	148/0	728/0	57/0	411/0
Hex-Ala w/Halo	200/0	523/0	80/0	543/0

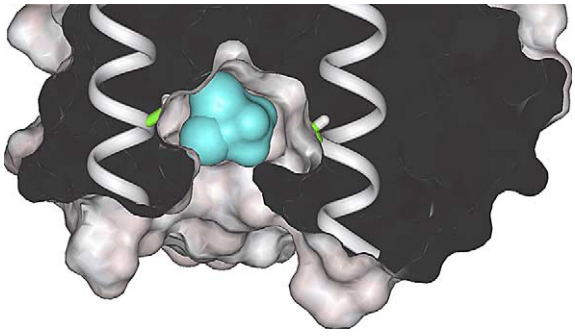

Fig. 2. Space-filling model of the halothane/Hex-Ala complex, generated using the Docking module (Section 2).

Table 2
Hydrogen–tritium exchange results

Peptide	$\Delta\Delta G$, kcal/mol
Hex-Ala	0.37 ± 0.11
Hex-Lys	0.00 ± 0.0
Hex-Phe	0.00 ± 0.0
Hex-Ile	−0.16 ± 0.04
DSD	0.00 ± 0.0

Values are means ± SEM, $n = 3$.

3.2. Hydrogen–tritium exchange

The results, expressed as $\Delta\Delta G$, are summarized in Table 2. As expected for Hex-Phe, nearly all of which is hexameric, baseline exchange rates were slow, and halothane had no detectable effect on these rates. Halothane also had no effect on the more rapid exchange rate of DSD or Hex-Lys, peptides that form hexamers less readily in solution. In the fully oligomerized Hex-Phe, halothane also had no effect on exchange rates (Fig. 3b, Table 2). On the other hand, for Hex-Ala at ~30 μM, where the dimer and hexamer are nearly equimolar, halothane decreased the exchange rate of slow amide protons (Fig. 3a and Table 2). For Hex-Ile, a peptide that is predominantly hexameric at the concentration of the experiment, halothane produced a slight *increase* in exchange rates, corresponding to a destabilization of ~0.16 kcal/mol (Table 2).

3.3. Analytical ultracentrifugation

In the peptide concentration range of the experiment, and in the absence of halothane, Hex-Ala exists in a dimer–hexamer equilibrium with a K_d of 2×10^{-10} M^2. In the presence of halothane, Hex-Ala sediments as a fully hexameric single species. The effect of halothane is evident in the raw data shown in Fig. 4. Given the range of concentrations explored in the experiment, we estimate that the K_d for the equilibrium must be lower than $\sim 1 \times 10^{-13}$ M^2. In contrast, the K_d similarly determined for the Hex-Lys mutant was 1.2×10^{-6} M^2, a value that did not change significantly with the addition of halothane. Thus, binding of halothane specifically to the Hex-Ala mutant shifts the dimer–hexamer equilibrium towards the hexamer by at least three orders of magnitude. This technique could not be used to investigate

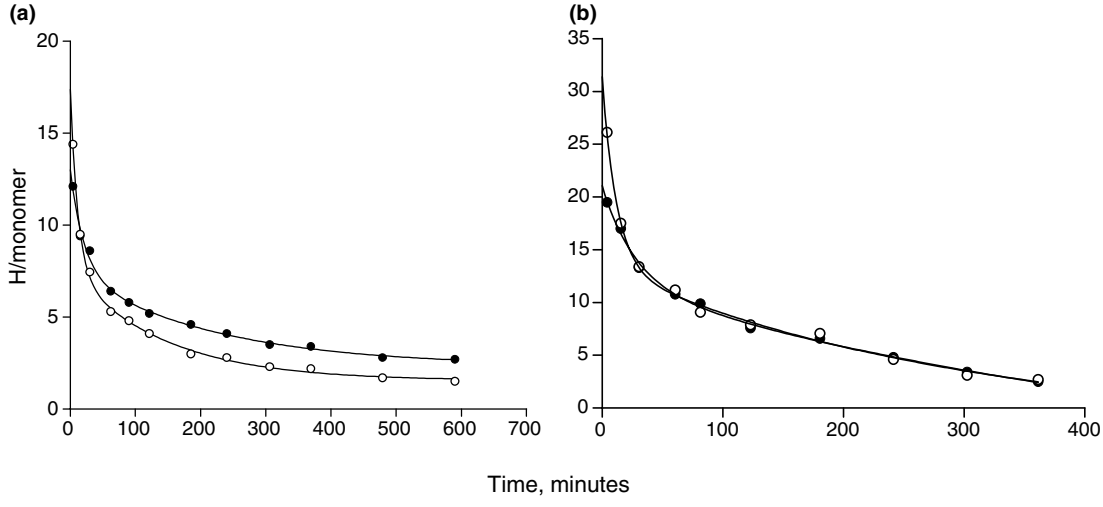

Fig. 3. Hydrogen–tritium exchange-out. (a) In Hex-Ala, halothane (7 mM) reduces slow amide hydrogen exchange. (b) In Hex-Phe, halothane (7 mM) had no detectable effect on slow hydrogen exchange rates. Filled symbols are halothane and open control. PFR values are a ratio of the time required for exchange-out of a given H under native conditions to that for the same H in the presence of the anesthetic. This is repeated for at least 3 of the slowest hydrogens for which there are data.

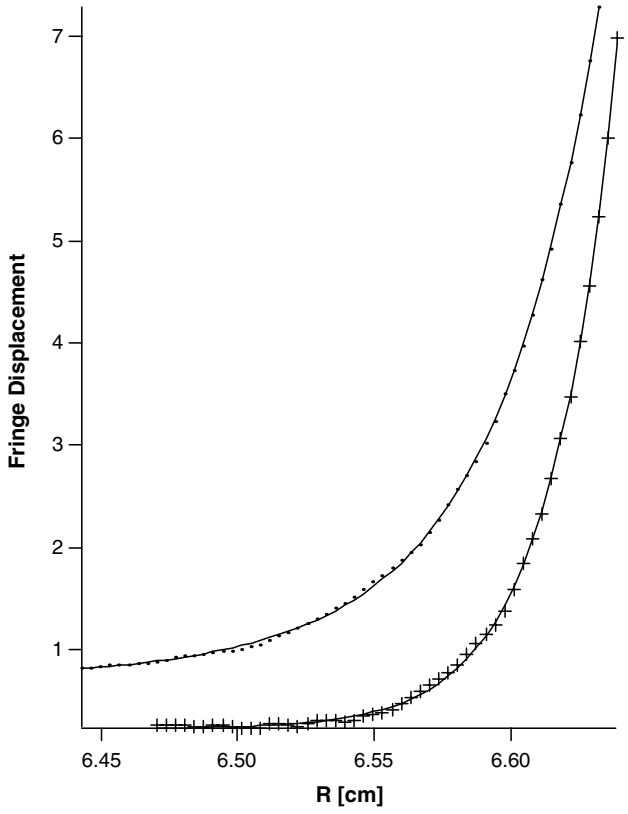

Fig. 4. Analytical ultracentrifugation data for Hex-Ala peptide as described in Section 2. Dots are without halothane and crosses are with halothane. Lines are fits to data as described in Section 3.

binding of halothane to Hex-Phe and Hex-Ile because these peptides have K_ds lower than 1×10^{-13} M^2, eliminating an ability to detect a further stabilization of the hexamer.

4. Discussion

We previously found that the number of aromatic residues in the "supercore" of the oligomeric assembly determines the aggregation state of the protein; while Hex-Ile and Hex-Phe form stable hexamers in solution, Hex-Lys and Hex-Ala exist in a dimer–hexamer equilibrium. The dissociation constant for hexamer (trimer of dimers) formation correlates with the polarity of side chain 42. The values calculated by analytical centrifugation are 1.2×10^{-7} M^2 for Hex-Lys and 6.3×10^{-10} M^2 for Hex-Ala, respectively [14].

While it was not possible to obtain an exact value for the Hex-Phe and Hex-Ile mutants, the K_ds are estimated to be lower than 10^{-13} M^2. Thus, only mutants that can form a well-packed supercore assemble into a stable hexamer. If assembly of the supercore produces packing defects, then the molecule exists in a dimer–hexamer equilibrium. This system provides an ideal model of allosteric regulation: in fact, the mutants populate different conformational states, dimer and hexamer, which are selectively stabilized for each mutant depending on the hydrophobic nature of a single residue.

We hypothesized that halothane would bind to apolar cavities at the top and bottom extremities of the Hex-Ala assembly, restoring van der Waals contacts lost by the mutation, thus shifting the dimer–hexamer equilibrium towards the hexamer. Molecular modeling of the hexameric mutants shows that halothane can only be accommodated within the Hex-Ala pocket(s). The SAV of these pockets is 59 $Å^3$ in Hex-Phe, 91 $Å^3$ in Hex-Ile, and 57 $Å^3$ in Hex-Lys. The SAV for Hex-Ala was 230 $Å^3$, but when occupied by halothane in our model, this volume is reduced to 80 $Å^3$, very similar to the other mutants. Thus, the ligand appears to bury a comparable hydrophobic surface, and we predicted rescue of the destabilizing mutation as has been observed for different ligands in other designed systems [18,19].

Centrifugation and hydrogen exchange experiments show that halothane stabilizes the Hex-Ala hexamer. The centrifugation experiments suggest a larger free energy change than that determined by HX, but the direct comparison requires that exchange-out occur only from the dimeric peptide and not from the hexameric, a situation known to be invalid. Both methods also clearly indicate the absence of stabilization of Hex-Lys, presumably because of an inadequate pocket volume, or the introduced full charge [9]. We used DSD, the parent peptide in the series, essentially unable to form hexamers in solution, as a control for the hydrogen exchange experiment. Halothane had no effect on HX exchange-out rates of DSD, indicating an absence of stabilization, and therefore binding, to the dimer. Therefore, the observed changes in HX rates for the other peptides are at least in part due to shifts in the oligomerization equilibria. Finally, HX data indicate an absence of stabilization and binding to Hex-Phe, presumably because of the predicted undersized cavity. Interestingly, molecular modeling predicts the volume of the Hex-Ile cavity to be slightly lower than the molecular volume of halothane, and HX indicates a destabilization. This suggests either binding to the dimer, or to a destabilized hexamer [20].

The ability of these small hydrophobic molecules to modulate protein oligomerization introduces a novel and potentially generalizable biophysical basis for inhaled anesthetic action. Suggested in the case of the CaATPase [11,12], modulation of oligomerization is directly demonstrated in this α-helical system. It is relevant that the transmembrane topology of the ligand-gated ion channels, plausible anesthetic targets, is thought to consist of α-helical bundles non-covalently assembled in the lipid bilayer. Moreover, a large fraction of interfacial pockets in protein complexes is uncomplemented by contiguous surface, providing the opportunity for small ligands to stabilize the complex [21]. Protein–protein interactions underlie much of biology and certainly signaling in the central nervous system. The widespread and diverse effects reported for the inhaled anesthetics, once thought to reflect the indirect effects of physical perturbations of lipid bilayers, may actually reflect more specific, but similarly widespread effects at protein–protein interfaces.

References

[1] Eckenhoff, R.G. and Johansson, J.S. (1997) Molecular interactions between inhaled anesthetics and proteins. Pharmacol. Rev. 49, 343–367.
[2] Campagna, J.A., Miller, K.W. and Forman, S.A. (2003) Mechanisms of actions of inhaled anesthetics. N. Engl. J. Med. 348, 2110–2124.
[3] Ishizawa, Y., Pidikiti, R., Liebman, P.A. and Eckenhoff, R.G. (2002) G protein-coupled receptors as direct targets of inhaled anesthetics. Mol. Pharmacol. 61, 945–952.

[4] Chiara, D.C., Dangott, L.J., Eckenhoff, R.G. and Cohen, J.B. (2003) Identification of nicotinic acetylcholine receptor amino acids photolabeled by the volatile anesthetic halothane. Biochemistry 42, 13457–13467.
[5] Bhattacharya, A.A., Curry, S. and Franks, N.P. (2000) Binding of the general anesthetics propofol and halothane to human serum albumin. High resolution crystal structures. J. Biol. Chem. 275, 38731–38738.
[6] Franks, N.P., Jenkins, A., Conti, E., Lieb, W.R. and Brick, P. (1998) Structural basis for the inhibition of firefly luciferase by a general anesthetic. Biophys. J. 75, 2205–2211.
[7] Eckenhoff, R.G. (1996) Amino acid resolution of halothane binding sites in serum albumin. J. Biol. Chem. 271, 15521–15526.
[8] Johansson, J.S., Eckenhoff, R.G. and Dutton, P.L. (1995) Binding of halothane to serum albumin demonstrated using tryptophan fluorescence. Anesthesiology 83, 316–324.
[9] Liu, R., Pidikiti, R., Ha, C.E., Petersen, C.E., Bhagavan, N.V. and Eckenhoff, R.G. (2002) The role of electrostatic interactions in human serum albumin binding and stabilization by halothane. J. Biol. Chem. 277, 36373–36379.
[10] Eckenhoff, R.G., Tanner, J.W. and Liebman, P.A. (2001) Cooperative binding of inhaled anesthetics and ATP to firefly luciferase. Proteins 42, 436–441.
[11] Kutchai, H., Geddis, L.M., Jones, L.R. and Thomas, D.D. (1998) Differential effects of general anesthetics on the quaternary structure of the Ca-ATPases of cardiac and skeletal sarcoplasmic reticulum. Biochemistry 37, 2410–2421.
[12] Glover, L., Heffron, J.J. and Ohlendieck, K. (2004) Increased sensitivity of the ryanodine receptor to halothane-induced oligomerization in malignant hyperthermia-susceptible human skeletal muscle. J. Appl. Physiol. 96, 11–18.
[13] Dzoljic, M., Bene, L., Krasznai, Z., Damjanovich, S. and Van Duijn, B. (2000) Ethanol and halothane differently modulate HLA class I and class II oligomerization. A new look at the mode of action of anesthetic agents through fluorescence spectroscopy. J. Photochem. Photobiol. 56, 48–52.
[14] Ghirlanda, G., Lear, J.D., Ogihara, N.L., Eisenberg, D. and DeGrado, W.F. (2002) A hierarchic approach to the design of hexameric helical barrels. J. Mol. Biol. 319, 243–253.
[15] Liang, J., Edelsbrunner, H. and Woodward, C. (1998) Anatomy of protein pockets and cavities:measurement of binding site geometry and implications for ligand design. Protein Sci. 7, 1884–1897.
[16] Richards, F.M. (1977) Areas, volumes, packing and protein structure. Annu. Rev. Biophys. Bioeng. 6, 151–176.
[17] Connolly, M.L. (1983) Solvent-accessible surfaces of proteins and nucleic acids. Science 221, 709–713.
[18] Gonzalez Jr., L., Plecs, J.J. and Alber, T. (1996) An engineered allosteric switch in leucine-zipper oligomerization. Nat. Struct. Biol. 3, 510–515.
[19] Doerr, A.J., Case, M.A., Pelczer, I. and McLendon, G.L. (2004) Design of a functional protein for molecular recognition: specificity of ligand binding in a metal-assembled protein cavity probed by 19f NMR. J. Am. Chem. Soc. 126, 4192–4198.
[20] Eckenhoff, R.G., Pidikiti, R. and Reddy, K.S. (2001) Anesthetic stabilization of protein intermediates: myoglobin and halothane. Biochemistry 40, 10819–10824.
[21] Li, X., Keskin, O., Ma, B., Nussinov, R. and Liang, J. (2004) Interfacial pockets, structurally conserved residues, and energetic hot spots in protein–protein interactions. Biophys. J. 1557-Pos/B542, 301a.